07 - 10 September 2009

PROCEEDINGS

54. IWK

Internationales Wissenschaftliches Kolloquium

International Scientific Colloquium

Information Technology and Electrical Engineering - Devices and Systems, Materials and Technologies for the Future

Faculty of Electrical Engineering and Information Technology

TECHNISCHE UNIVERSITÄT
ILMENAU

Impressum

Herausgeber: Der Rektor der Technischen Universität Ilmenau
Univ.-Prof. Dr. rer. nat. habil. Dr. h. c. Prof. h. c.
Peter Scharff

Redaktion: Referat Marketing
Andrea Schneider

Fakultät für Elektrotechnik und Informationstechnik
Univ.-Prof. Dr.-Ing. Frank Berger

Redaktionsschluss: 17. August 2009

Technische Realisierung (USB-Flash-Ausgabe):
Institut für Medientechnik an der TU Ilmenau
Dipl.-Ing. Christian Weigel
Dipl.-Ing. Helge Drumm

Technische Realisierung (Online-Ausgabe):
Universitätsbibliothek Ilmenau
ilmedia
Postfach 10 05 65
98684 Ilmenau

Verlag: isle
Verlag ISLE, Betriebsstätte des ISLE e.V.
Werner-von-Siemens-Str. 16
98693 Ilmenau

ISBN (USB-Flash-Ausgabe): 978-3-938843-45-1
ISBN (Druckausgabe der Kurzfassungen): 978-3-938843-44-4

Startseite / Index:
http://www.db-thueringen.de/servlets/DocumentServlet?id=14089

CONTRIBUTION TO THE SIMULATION OF FREE SURFACE FLOWS IN ELECTROMAGNETIC FIELD

Ovidiu Peşteanu[1] *and Egbert Baake*[2]

[1] Department of Electrical Engineering, Transilvania University of Braşov,
B-dul Eroilor 29, RO-900036 Braşov, Romania
[2] Institute of Electrotechnology, Leibniz University of Hanover,
Wilhelm-Busch-Str. 4, D-30167 Hanover, Germany

ABSTRACT

A strictly mass conserving VOF method based on the advection of a local height function, which was used e.g. for water impact problems, is applied also for the simulation of MFD free surface flows. Specific stress and pressure boundary conditions are employed at the melt free surface. An experimental validating of the method was obtained by the good agreement of the calculated free surface form with the measurements performed in a laboratory induction coreless furnace.

Index Terms – MFD free surface flow, finite difference method, VOF method, local height function, pressure at melt surface in electromagnetic field

1. INTRODUCTION

One of the most popular method for the simulation of unsteady free surfaces is the Volume Of Fluid (VOF) method based on the advection of a VOF function F [1], indicating the fractional volume of a computational cell filled with fluid, i.e. $F = 0$ in the empty cells E (**Fig. 1**), $0 < F < 1$ in the adjacent partly filled surface cells S and $F = 1$ in the completely filled fluid cells F, respectively. After every calculation time step, the free surface can be reconstructed using a Simple Line Interface Construction (SLIC) [1, 2] or a more accurate method employing a Piecewise Linear Interface Construction (PLIC) [3–5].

The applying of the donor-acceptor [1] and PLIC methods [3, 4] can yield values $F < 0$ or $F > 1$ and by their rounding to 0 and 1, respectively, the volume conservation of an incompressible fluid is destroyed. Another drawback of these methods is the numerical creation of unphysically holes in the fluid or of 'flotsam' and 'jetsam', which are small droplets disconnected from the free surface [2−4].

To avoid these disadvantages, the VOF method was combined with a Local Height Function (LHF) [6] and successfully employed for the simulation of the coupled solid-liquid dynamics under extra-terrestrial conditions in spacecraft [7], of water waves impact problems [8, 9] and two-phase flows in sloshing tanks [10], respectively.

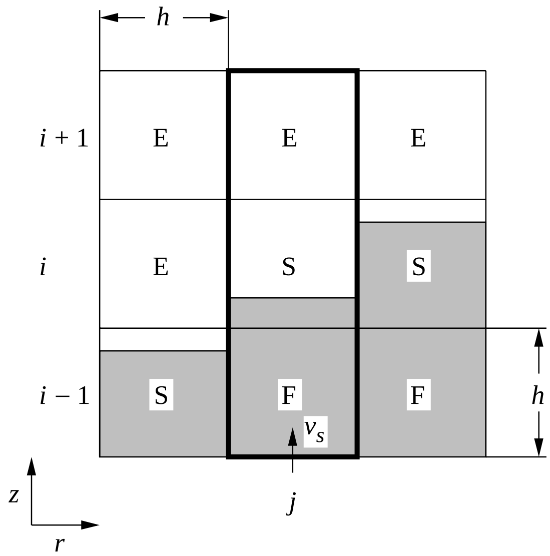

Fig. 1. Cell labeling and block for defining the LHF.

In this paper, the VOF method combined with a LHF is extended to the simulation of electromagnetically driven free surface flows by introduction of the followings:

- Proper calculation of the electromagnetic field and pressure in S cells [11]
- Volume conserving displacement of the melt free surface by advection of a dimensionless LHF

By using the Finite Difference Method (FDM), the extended MagnetoFluidDynamic (MFD) LHF-VOF method was implemented in a self-developed computational program and employed for the flow modeling in an Induction Crucible Furnace (ICF) [12], the calculated free surface showing a good agreement with the measurements presented in [13].

2. ELECTROMAGNETIC FIELD COMPUTATION

The electromagnetic field is determined by solving the conservative differential equations of the magnetic vector potential for the points of a staggered grid. Thus, the finite difference equations approximate more accurately the Ampère's circuital theorem [14].

In cylindrical coordinates r, φ, z, the conservative equations of the vector potential **A** are given in [14] for non-ferromagnetic media and in [15] for the presence of magnetic cores, respectively. In these equations, all terms preserve the conservative property also in radial direction, e.g. the following term must be used in the equation of component A_r [14]:

$$T = -\frac{1}{r^2}\frac{\partial}{\partial r}(r A_\varphi) + \frac{\partial}{\partial r}\left(\frac{1}{r}\frac{\partial A_\varphi}{\partial \varphi}\right) \qquad (1)$$

instead of the more simple, but non-conservative

$$T = -\frac{2}{r^2}\frac{\partial A_\varphi}{\partial \varphi}. \qquad (2)$$

According to the reasons explained in [11], in order to obtain a realistic MFD simulation, the partly filled surface cells must be considered in the electromagnetic calculations as being completely filled with melt. Thus, both the electromagnetic and force fields are computed in the S cells using the whole electrical conductivity σ of the molten metal, instead of the usually reduced conductivity $F\sigma$.

3. CALCULATION OF TURBULENT FLOW

The flows in industrial induction applications are most accurately calculated using the method of Large Eddy Simulation (LES) [16, 17]. For flows characterized by very low frequencies of the large scale velocity oscillations, whose modeling with LES requires excessive time and computational resources [16], the computationally less expensive k-ε or Reynolds stress models [18, 19] can be applied.

For known Lorentz forces, all FF, FS and SS velocities are first determined by the explicitly discretised momentum equations, considering all F and S cells to be completely filled with fluid [7–9]. Afterwards, the SOLution Algorithm (SOLA) [1, 20] is employed for the iterative correction of pressure and velocity fields to satisfy continuity in all F cells [11]. Finally, the turbulence field is computed in all F and S cells, e.g. k and ε are calculated from their discretised transport equations.

The Quadratic Upstream Interpolation for Convective Kinematics (QUICK) is applied in the momentum equations utilizing the flux-splitting procedure [21], excepting the near-wall and near-surface grid points, where in normal direction only the upwind scheme can be employed. In the equations of the turbulence field, the convective terms are approximated only by the upwind scheme.

To obtain greater maximal admissible time steps for the simulations in cylindrical coordinates, the diffusive terms in φ-direction are treated implicitly and all other terms explicitly [22, 23]. In case of rotational flows, the known near-middle velocity increase in the flow-mechanically stable layers can be modeled by using either the Reynolds stress model or nonisotropic versions of the k-ε model [21] and the Smagorinsky model in LES [23], respectively.

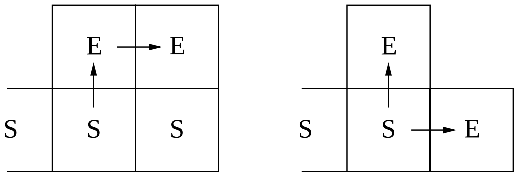

Fig. 2. Configurations of SE and EE velocities.

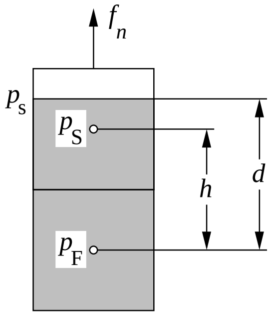

Fig. 3. Concerning the pressure calculation in S cells.

4. FREE SURFACE BOUNDARY CONDITIONS

Generally, an electric potential is used in the equations of the magnetic vector potential, to annul the normal current density at the conductor surface.

The stress and pressure boundary conditions will be briefly presented for the upper surface of an axisymmetric flow with the velocity components u and v in the r- and z-directions.

Because of the reasons explained in [11], the discretised continuity equation is employed in all S cells. The equation can be applied immediately, where the SE velocity follows from the other three always calculated velocities (**Fig. 2** left) and subsequently, the upper EE velocity is determined from the discretised tangential stress condition [7, 8]

$$\frac{\partial u}{\partial z} + \frac{\partial v}{\partial y} = 0. \qquad (3)$$

In case of an S cell with two open sides, which are not positioned opposite each other (Fig. 2 right), the conservation of velocity component v in z-direction is supplementary demanded [7].

If the free surface lies between the central points of two neighboring F and S cells, then the pressure is extrapolated in the S cell as (**Fig. 3**) [1]

$$p_S = \eta p_s + (1-\eta) p_F \quad \text{if } d \le h,$$
$$\eta = \frac{d}{h}, \quad p_s = p_a + p_\gamma + 2\mu_{\text{eff}}\frac{\partial v}{\partial z}, \qquad (4)$$

where p_a, p_γ and μ_{eff} represent the ambient pressure, the pressure due to the surface tension γ and the effective dynamic viscosity, respectively.

For an S cell's centre located below the surface, the pressure may be determined more accurately considering the variable space-distribution of the electromagnetic force density by [11]

$$p_S = p_s - (d-h) f_n \quad \text{if } d > h, \qquad (5)$$

Table 1. Calculation of VOF functions.

H	$F_{i-1,j}$	$F_{i,j}$	$F_{i+1,j}$
$H < 1 - e$	H	0	0
$1 + e < H < 2 - e$	1	$H - 1$	0
$H > 2 + e$	1	1	$H - 2$

where f_n denotes the resulting normal force density acting on the cell's upper face (Fig. 3).

In a new S cell appeared in a transient flow simulation, the physical quantities of the turbulence field from its southern cell are set as initial values, e.g. the values of k, ε, μ_{eff} and, in case of a near-wall S cell, also of the friction velocity, when using the k-ε turbulence model [11].

5. FREE SURFACE DISPLACEMENT

The free surface advection and reconstruction will be presented also for the upper surface of an axisymmetric flow. For every S cell i, j (Fig. 1), a dimensionless LHF is introduced for the free surface treatment, defined when using an uniform grid by [1, 7−10]

$$H = \sum_m F_{m,j}, \tag{6}$$

where the summation is from $m = i - 1$ to $m = i + 1$.

During a calculation time step Δt, the conservation of the melt volume in the thick line column shown in Fig. 1 may be expressed as

$$(H^{\text{new}} - H)V_j + \sum_m (\Phi_{em} - \Phi_{wm}) - V_s = 0, \qquad V_j = r_j\, h^2, \quad V_s = v_s\, \Delta t\, r_j\, h, \tag{7}$$

in which V_j and h represent the volume (modulo 2π) corresponding to the cell i, j of mean radius r_j and the grid size, respectively, and v_s denotes the velocity across the southern side of the three-cell block.

In Eq. (7), the terms Φ_{em} and Φ_{wm} indicate the radial fluxes (modulo 2π) through the eastern and western faces of cell m, j calculated by

$$\Phi = r_f\, u_f\, \Delta t\, h\, F_P, \tag{8}$$

where r_f and u_f are the radius of the cell face and the velocity passing through it, respectively, while F_P denotes the VOF value from adjacent grid point P to the considered face on its upstream side.

By using a stability limited time step Δt in the explicit Eqs. (7) and (8), no overflow $H > 3$ or underflow $H < 0$ of the column can occur and therefore, the method is strictly volume conserving [6−10]. The three individual VOF values in the column j (Fig. 1) are determined from the new calculated H value according to **Table 1**, where a small constant e was introduced to prevent numerically generated oscillations of the VOF values, i.e. of the computed free surface.

Finally, the free surface is reconstructed as a stepped curve using the known SLIC [1, 7−10].

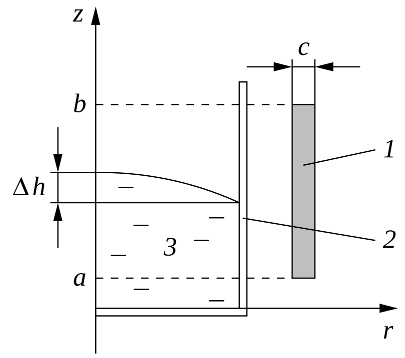

Fig. 4. Transverse section of test furnace (schematic): *1* – inductor, *2* – crucible, *3* – melt.

Table 2. Characteristics of the ICF (Fig. 4) [12, 13]

frequency, r.m.s. value of the inductor current	386 Hz I = 2 kA
inner diameter of the inductor	385 mm
inferior and superior heights of the copper tube inductor	a = 47.5 mm b = 570 mm
wall thickness of the copper tube	c = 3.5 mm
inner diameter of crucible	316 mm
mean height of Wood's metal melt	400 mm
physical properties of molten Wood's metal	9.4 kg/dm^3 σ = 1 MS/m μ = 4.2 cP γ = 0.46 N/m

6. RESULTS

The transient MFD field was simulated in a test ICF (**Fig. 4**) described in **Table 2** [12, 13], using the k-ε model. By the partially filling of the nonmagnetic steel crucible with molten Wood's metal, an intensive turbulent flow was electromagnetically driven in the laboratory furnace [13], which is suitable for experimental verifications of flow calculations.

The presented MFD LHF-VOF method is not used in the commercial codes available for the electromagnetic field and flow simulations. Therefore the method was implemented in a self-developed computational program in FORTRAN, by applying the FDM for a 40 x 120 grid in the r- and z- directions, destined for two-dimensional (2D) MFD simulations.

The n = 11 series turns of the inductor were considered in the electromagnetic field computation as being fed at $t \geq 0$ with a sinusoidal current of constant r.m.s. value I (Table 2). In Fig. 4, *1* represents only the inner walls of the inductor's copper tube with rectangular profile. The magnetic vector potential was determined assuming that the total current nI of the inductor is distributed only over these inner walls with a density equal to (Fig. 4):

$$J = \frac{nI}{(b-a)c} = 12\,\frac{\text{A}}{\text{mm}^2}. \tag{9}$$

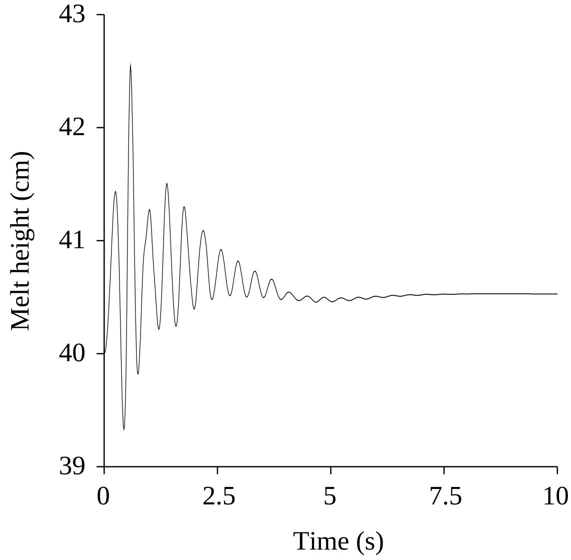

Fig. 5. Calculated transient melt height at $r = 0$.

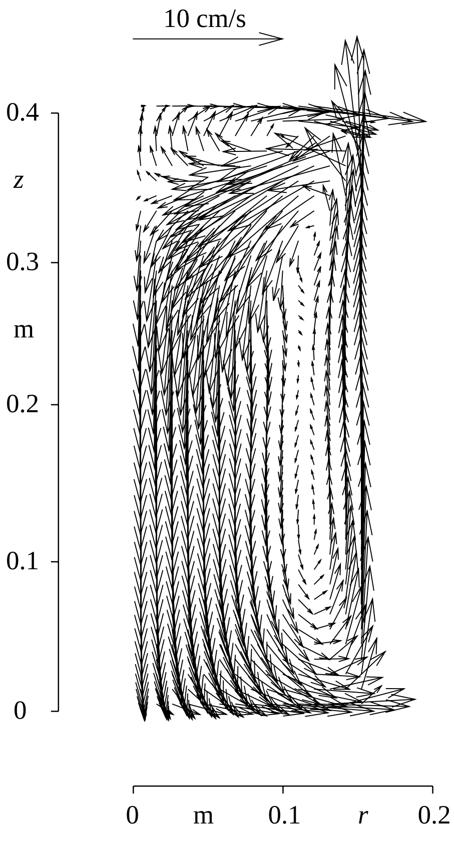

Fig. 6. Calculated velocity distribution at $t = 20$ s.

A calculated evolution in time of the middle bath height is shown in **Fig. 5**, where final unphysically oscillations of the melt height were removed by using the value $e = 10^{-4}$ for the small adjusting constant introduced in Table 1. The steady flow, determined in the MFD simulation as the final solution at $t = 20$ s of the transient flow, is characterized, as in the measurements [13], by one very large eddy (**Fig. 6**).

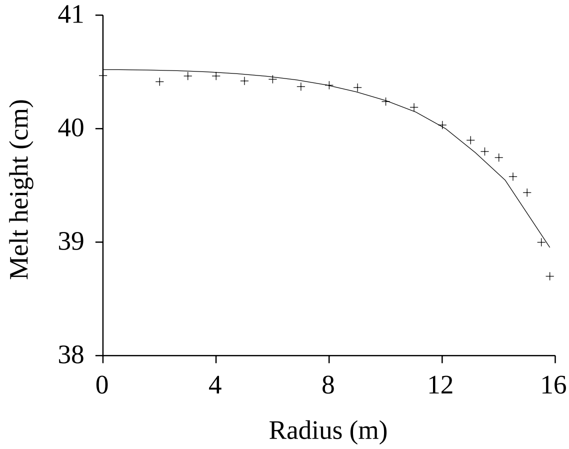

Fig. 7. Free surface profile: symbols – measured values [13], line – calculated curve at $t = 20$ s.

An experimental validating of accuracy in the free surface calculation by the presented MFD simulation was obtained as follows.

From the visually determined melt heights using a contact method (**Fig. 7**) [13], results a bath level difference Δh (Fig. 4) of the strongly deformed free surface in the partly filled crucible of $\Delta h = 17.5{-}18$ mm.

By utilization of the commercial ANSYS package for the 2D computation of the steady electromagnetic field, Lorentz forces, flow field and free surface by applying the stationary k-ε model and the classical VOF method, wavy surface shapes were calculated in [13] with a deformation of about $\Delta h = 7$ mm, which is more than two times lower comparing to the experimentally measured height difference.

With the presented MFD simulation, implemented with the unsteady k-ε model in the self-developed computer program, a smooth free surface profile with a more accurately calculated bath level difference of $\Delta h = 15.7$ mm was determined (Fig. 7).

7. REFERENCES

[1] C.W. Hirt, and B.D. Nichols, "Volume of Fluid (VOF) Method for Dynamics of Free Boundaries," *J. Comp. Phys.*, vol. 39, pp. 210–225, 1981.

[2] W.F. Noh, and P. Woodward, " SLIC (simple line interface calculation)," in *Lecture Notes in Physics*, *Proc. Fifth Int. Conf. on Numer. Meth. Fluid Dynamics*, vol. 59, A.I. van de Vooren, and P.J. Zandbergen, eds., Springer, New York, pp. 330–340, 1976.

[3] M. Rudman, "Volume-tracking methods for interfacial flow calculations," *Int. J. Numer. Meth. Fluids*, vol. 24, pp. 671–691, 1997.

[4] W.J. Rider, and D.B. Kothe, "Reconstructing volume tracking," *J. Comp. Phys.*, vol. 141, pp. 112–152, 1998.

[5] P. Liovic, J.-L. Liow, and M. Rudman, “A volume of fluid (VOF) method for the simulation of metallurgical flows,” *ISIJ Int.*, vol. 41, pp. 225−233, 2001.

[6] Z.A. Sabeur, J.E. Cohen, J.R. Stephens, and A.E.P. Veldman, “Investigation on free surface flow oscillatory impact pressures with the Volume of Fluid method,” in *Numer. Meth. Fluid Dynamics VI*, M.J. Baines, ed., Will Print, Oxford, pp. 493−498, 1998.

[7] J. Gerrits, Dynamics of liquid-filled spacecraft, Ph.D. Thesis, University of Groningen, 2001.

[8] K.M.T. Kleefsman, Water impact loading on offshore structures, Ph.D. Thesis, University of Groningen, 2005.

[9] K.M.T. Kleefsman, G. Fekken, A.E.P. Veldman, B. Iwanowski, and B. Buchner, “A Volume-of-Fluid based simulation method for wave impact problems,” *J. Comp. Phys.*, vol. 206, pp. 363−393, 2005.

[10] R. Wemmenhove, R. Luppes, A.E.P. Veldman, and T. Bunnik, “Application of a VOF method to model compressible two-phase flow in sloshing tanks,” in *Proc. 27th Int. Conf. Offshore Mechanics and Arctic Eng.*, Estoril, paper OMAE2008-57254, 2008.

[11] O. Peşteanu, “Contribution to the application of the SOLA-VOF method for MFD flows,” these proceedings, Electro-Processing Technologies, 2009.

[12] E. Baake, Grenzleistungs- und Aufkohlungsverhalten von Induktions-Tiegelöfen, Düsseldorf, VDI, 1994.

[13] M. Kirpo, Modeling of turbulence properties and particle transport in recirculated flows, Ph.D. Thesis, University of Latvia, Riga, 2008.

[14] O. Peşteanu, E. Baake, and B. Nacke, “Induktives Schwebeschmelzen mit zwei Frequenzen,” in *Proc. Workshop Elektroprozesstechnik*, TU Ilmenau, Rep. 8, 2004.

[15] O. Peşteanu, “Erzeugung räumlich einstellbarer Kraftdichteverteilungen und Strömungsfelder beim elektromagnetischen Rühren von Metallschmelzen,” Report of DFG-Project SCHW 176/36-1, 2007.

[16] E. Baake, B. Nacke, A. Umbrashko, and A. Jakovics: “Transient 3D Simulation of Recirculated Melt Flow,” in *Proc. Int. Sci. Colloquium Modelling for Saving Resources*, Riga, pp. 129−134, 2001.

[17] E. Baake, A. Umbrashko, and A. Jakovics: “Modeling of the turbulent melt flow in metallurgical processes,” CD-ROM of *51st Int. Sci. Colloquium*, Ilmenau, Electro-Processing Technologies, 2006.

[18] R. Schwarze, and F. Obermeier, “Modelling of unsteady electromagnetically driven recirculating melt flows,” *Modelling Simul. Mater. Sci. Eng.*, vol. 12, pp. 985−993, 2004.

[19] R. Schwarze, “Unsteady RANS simulation of oscillating mould flows,” *Int. J. Numer. Meth. Fluids*, vol. 52, pp. 883−902, 2006.

[20] U. Brockmeier, Numerisches Verfahren zur Berechnung dreidimensionaler Strömungs- und Temperaturfelder in Kanälen mit Längswirbelerzeugern und Untersuchung von Wärmeübergang und Strömungsverlust, Ph.D. Thesis, Ruhr University of Bochum, 1987.

[21] O. Peşteanu, and K. Schwerdtfeger, “Einstellung der Kraftdichteverteilung und des Strömungsfeldes beim elektromagnetischen Rühren von Metallschmelzen,” CD-ROM of *48th Int. Sci. Colloquium*, Ilmenau, Electro-Processing Technology, 2003

[22] J.G.M. Eggels, Direct and large eddy simulation of turbulent flow in cylindrical pipe geometry. Ph.D. Thesis, Technical University Delft, 1994.

[23] O. Peşteanu, and K. Schwerdtfeger, “Contribution to the large eddy simulation of flows in electromagnetic stirrers for continuous casting,” *ISIJ Int.*, vol. 43, pp. 1556−1561, 2003.